Journal of Engineering Mathematics, Vol. 12, No. 2, April 1978
Sijthoff & Noordhoff International Publishers–Alphen aan den Rijn
Printed in The Netherlands

Heat or mass transfer from an open cavity

H. K. KUIKEN

Philips Research Laboratories, Eindhoven, The Netherlands

(Received May 26, 1977)

SUMMARY

This paper presents a mathematical model for heat or mass transfer from an open cavity. It is assumed that the Péclet number, based on conditions at the cavity, and the Prandtl number are both large. The model assumes heat- or mass-transfer boundary layers at the rim of the cavity vortex flow. Heat or mass exchange with the surrounding fluid occurs in a free boundary layer which spans the mouth of the cavity. It is shown that the solution depends upon a single parameter ω only. This parameter is determined by the flow field. For small and large values of ω matched asymptotic expansions are presented. The model is illustrated for a few simple flows in closed cavities. Etching, clot formation in flowing blood, lubrication and cooling of rough surfaces are mentioned as possible fields of application.

1. Introduction

Several reasons can be given for the considerable attention that has been paid in the literature to flows past open cavities and cut-outs, especially when seen in connection with the transfer of heat or mass. Reiman and Sabersky [1] mention that heat transfer from rough surfaces can be understood more completely when the transfer of heat from cavities has been studied. It is clear that the transfer of heat from cavities plays an important part in the fields of bearing lubrication and turbine flow. A rather interesting application in the field of biomechanics was given in a recent study by Stevenson [2]. This author suggested that clot formation in flowing blood (thrombogenesis) might be explained by a study of mass transfer from open cavities that may exist in the artery wall. Surface reactions at the cavity wall may produce certain materials, which remain trapped in the vortex that exists in the cavity. A high concentration of these materials could lead to thrombogenesis. Other applications, particularly in the field of aerodynamics can be found in a review paper by Chilcott [3].

The present study was motivated by a desire to obtain a better understanding of certain etching processes. The problem put before us was that the etching process is strongly dependent upon the size of the orifice of the cavity (Goosen and Van Ruler [4]). These authors did an experiment in which pure etchant was forced to flow along a surface in which minute cavities were embedded. It was noticed that initially the etching speed was independent of the cavity size. However, when etching had gone down to a depth which is comparable to the width of the orifice of the cavity, the etching proceeded at a speed that was noticeably less than the initial speed. In the experiments conducted by Goosen and Van Ruler the Reynolds number, based on the size of the cavity, was moderate, whereas the

Péclet number was very large. We may therefore expect that the transfer processes are restricted to a mass-transfer boundary layer near the wall of the cavity. Following a similar heat-transfer model, which seems to have been considered first in some detail by Miles [5] and which is also described in a paper by Fenton and White [6], there is a free mass-transfer boundary layer which spans the mouth of the cavity and through which a convective and diffusive exchange of impure etchant takes place with the surrounding fluid. In this model the transfer of heat or mass is restricted to the rim of the cavity vortex flow. In the bulk of the vortex the impurities are distributed uniformly. This model is supported by numerical experiments on heat transfer in a driven cavity (Burggraf [7], Spalding et al. [8]). The analogous case of vorticity transfer in closed-streamline flows was considered by Batchelor [9].

If the cavity becomes deep enough, a second vortex will emerge near the bottom of the cavity (Pan and Acrivos [10]). Using the mass-transfer boundary-layer model described above we may now understand the decrease in etching speed. Indeed, the materials etched away in the lower reaches of the cavity have to circulate round two vortices before an exchange with the surrounding fluid can take place. We may also expect that the uniform concentration within the core of the lower vortex will be higher than when only one vortex is present. This will lower the concentration gradients down in the cavity.

In this paper we shall formulate our problem in terms of heat transfer with a fixed cavity wall. In a mass-transfer problem the cavity becomes gradually eroded, but this process seems to be slow enough to justify a quasi-steady approach. In that case a formulation in terms of heat transfer is analogous to that in terms of a concentration, but the first seems to be in more general use. Of course, the heat-transfer results can be translated directly into their mass-transfer analogue. The analysis will be restricted to two-dimensional cavities and we shall consider the case of a single vortex only.

Miles's approach to heat exchange from a cavity vortex was to consider the total heat transfer from the cavity wall to the wall boundary layer and to translate this into a line source of heat at the separation lip, i.e. at the leading edge of the free boundary layer. The total heat transfer is then considered to be the sum of two separate forms of heat transfer. The first is that obtained from the boundary layer resulting from the line source and of course only that part is considered which leaves the cavity at the free-stream side of the re-attachment point. The second factor contributing to heat transfer is the flow of heat from the bulk to the free stream.

In our analysis we shall improve upon these older ideas in that we shall attempt to establish a more realistic link between the two boundary layers. This means that we shall abandon the line-source idea and replace it by a rule which transforms the final temperature profile of the wall boundary layer into the initial one of the free boundary layer. Conversely, there will be a close connection between the final temperature profile of the free boundary layer and the initial one of the wall boundary layer. This process is greatly facilitated by the fact that we consider fluids with a large Prandtl number (or Schmidt number in the case of etching). We may then use a very simple velocity field to describe the convective terms in the boundary-layer equations. For this very reason the formulation of the problem is independent of the Reynolds number.

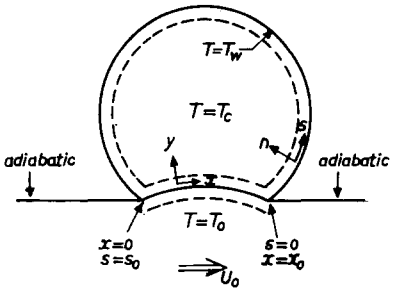

Figure 1. Geometrical model of an open cavity.

2. The mathematical model

Fig. 1 may serve as a model of a two-dimensional cavity, i.e. a depression in an otherwise smooth surface. A fluid flows along this surface, but the exact nature of this flow does not interest us here. All we need to know is that u_0 is a velocity characteristic for this flow. Under very general conditions the steady state reveals a trapped circulatory flow inside this cavity. The streamline separating this vortex from the outer flow is given in Fig. 1. The exact location of the point of attachment of the dividing streamline has been a matter of serious discussion in the literature. However, most of this literature refers to rectangular cut-outs. In general terms, the following picture transpires. For large Reynolds numbers the dividing streamline connects the edges of the cavity. For small Reynolds numbers there does not seem to be complete agreement. Takematsu's paper [11] on the slow viscous flow past a cavity of infinite depth arrives at the conclusion that the flow separates inside the cavity at a point beyond but rather close to the edge. A numerical study by Stevenson [2] on cavities of finite depth seems to confirm this conclusion. O'Brien [12] on the other hand leaves the matter undecided owing to loss of accuracy in the numerical procedure which she employed. Macagno and Hung [13], considering the flow in an expanding conduit find separation at the edge.

Be this as it may, in this paper we shall carry out the analysis assuming separation at the edges of the cavity. In the case of cusped edges this seems to be a reasonable assumption. Later we shall outline a modification to our analysis which covers the alternative separation phenomena, including the case of multiple separation occurring in deep cavities or in cavities with sharp internal corners.

To describe the temperature boundary layer along the dividing stream line, we use a coordinate system (x, y), where x measures the distance along and y the distance normal to the dividing stream line. If the velocity distribution along $y = 0$ is given by $u = u(x)$ we can write the equation for heat transport as

$$u(x)\frac{\partial T}{\partial x} - yu'(x)\frac{\partial T}{\partial y} = \kappa\frac{\partial^2 T}{\partial y^2}, \tag{2.1}$$

where we have used the fact that the Prandtl number is much larger than unity. Indeed, if Pr is large, temperature variations are much larger than velocity variations, so that we may use an approximate representation of the velocity field. We have to find a solution to this

equation in the region $0 \leqslant x \leqslant x_0, -\frac{1}{2}\delta_y < y < \frac{1}{2}\delta_y$. Here δ_y formally represents the thickness of the free boundary layer.

Along the wall of the cavity we use the coordinate system (s, n) with $0 \leqslant s \leqslant s_0$, $0 \leqslant n < \delta_n$. Again using the condition $Pr \gg 1$ we write the energy equation as

$$\alpha(s)n\frac{\partial T_i}{\partial s} - \tfrac{1}{2}\alpha'(s)n^2\frac{\partial T_i}{\partial n} = \kappa\frac{\partial^2 T_i}{\partial n^2}, \tag{2.2}$$

where $\alpha(s)$ is the normal derivative of the longitudinal velocity evaluated at $n = 0$. We use T_i to denote the temperature inside the wall boundary layer.

The boundary conditions are

$$T_i = T_w \quad \text{at} \quad n = 0, \qquad 0 \leqslant s \leqslant s_0, \tag{2.3}$$

$$\frac{\partial T_i}{\partial n} = 0 \quad \text{if} \quad n = \delta_n, \qquad 0 \leqslant s \leqslant s_0, \tag{2.4}$$

$$\frac{\partial T}{\partial y} = 0 \quad \text{if} \quad y = \tfrac{1}{2}\delta_y, \qquad 0 \leqslant x \leqslant x_0, \tag{2.5}$$

$$T = T_0 \quad \text{if} \quad y = -\tfrac{1}{2}\delta_y, \qquad 0 \leqslant x \leqslant x_0. \tag{2.6}$$

In addition to these boundary conditions we need to establish a connection between the two boundary layers, i.e. the initial condition at $x = 0$ must somehow be related to the end condition at $s = s_0$. At the location where $x = x_0$ and $s = 0$ a similar situation exists. It is common practice in boundary-layer theory not to bother too much about conditions at the leading edge, the reason being that downstream the influence of the initial condition becomes increasingly smaller. It is the wall conditions that determine boundary-layer behaviour. In the absence of wall conditions, as is the case with jets and free boundary layers, or in the case of inactive wall conditions, e.g. an adiabatic wall, the preservation of an overall quantity, such as total momentum or total heat, determines the boundary layer. The precise distribution of this quantity at the leading edge is of secondary importance.

It would seem that such an approach will be inadequate here. Indeed, the boundary layers considered here are of finite length. Moreover, the flow is periodic so that a true "downstream" does not exist. We therefore feel that it will be necessary to use a temperature profile at the leading edges of each of the boundary layers. A complete answer to this problem can only be obtained by a detailed study of the flow and heat transfer characteristics near the edge of the cavity. However, this appears to be far too complicated. The next best thing will be to relate the temperature profile just before the leading edge to that immediately past it. Since the flow field changes very rapidly near the edges of the cavity, it is not unreasonable to assume that the temperature remains constant along the streamlines in that region. This leads to the relations

$$T_i(s, n) \sim T(x, y); \ \tfrac{1}{2}\alpha(s)n^2 = u(x)y \ \text{ if } \ \frac{s_0 - s}{s_0} \ll 1 \ \text{ and } \ \frac{x}{x_0} \ll 1, \tag{2.7}$$

$$T(x, y) \sim T_i(s, n); \ u(x)y = \tfrac{1}{2}\alpha(s)n^2 \ \text{ if } \ \frac{x_0 - x}{x_0} \ll 1 \ \text{ and } \ \frac{s}{s_0} \ll 1. \tag{2.8}$$

From the definition of (2.7) and (2.8) it is clear that these conditions apply only in the region $y \geqslant 0$. To complete the set of boundary conditions we must therefore put

$$T(0, y) = T_0 \quad \text{if} \quad -\infty < y < 0. \tag{2.9}$$

The problem is now to solve the system consisting of the equations (2.1)–(2.9).

3. Solution

Let us introduce the following transformations. In the region $0 \leqslant x \leqslant x_0$ we have

$$T = T_0 + (T_w - T_0)\vartheta(X, Y), \tag{3.1}$$

$$X = \left\{\int_0^x u(p)dp\right\} X_0^{-1}, \tag{3.2}$$

$$Y = yu(x)(\kappa X_0)^{-\frac{1}{2}}, \tag{3.3}$$

$$X_0 = \int_0^{x_0} u(p)dp, \tag{3.4}$$

and in the region $0 \leqslant s \leqslant s_0$ we have

$$T_i = T_0 + (T_w - T_0)\theta(S, N), \tag{3.5}$$

$$S = \left\{\int_0^s \alpha^{\frac{1}{2}}(p)dp\right\} S_0^{-1}, \tag{3.6}$$

$$N = \alpha^{\frac{1}{2}}(s)n(\kappa S_0)^{-\frac{1}{2}}, \tag{3.7}$$

$$S_0 = \int_0^{s_0} \alpha^{\frac{1}{2}}(p)dp. \tag{3.8}$$

Using these transformations we can easily write the system (2.1)–(2.6) as

$$\frac{\partial \vartheta}{\partial X} = \frac{\partial^2 \vartheta}{\partial Y^2} \qquad (0 \leqslant X \leqslant 1, \ -\infty < Y < \infty),$$

$$\vartheta \to 0 \qquad \text{if} \quad Y \to -\infty, \tag{3.9}$$

$$\frac{\partial \vartheta}{\partial Y} \to 0 \quad \text{if} \quad Y \to \infty.$$

It is the largeness of the Péclet number which allows us to use $\pm\infty$ as upper and lower bounds. Further we have

$$N\frac{\partial\theta}{\partial S}=\frac{\partial^2\theta}{\partial N^2}\qquad(0\leqslant S\leqslant 1,\ 0\leqslant N<\infty),$$

$$\theta=1\quad\text{if } N=0, \tag{3.10}$$

$$\frac{\partial\theta}{\partial N}\to 0\quad\text{if } N\to\infty.$$

The patching conditions (2.7) and (2.8) are transformed into

$$\theta(S,N)=\vartheta(X,\omega N^2)\quad\text{if } (1-S)\ll 1 \text{ and } X\ll 1, \tag{3.11}$$

$$\vartheta(X,\omega N^2)=\theta(S,N)\quad\text{if } (1-X)\ll 1 \text{ and } S\ll 1, \tag{3.12}$$

and there does not seem to be any objection to replacing these by

$$\theta(1,N)=\vartheta(0,\omega N^2);\quad\vartheta(1,\omega N^2)=\theta(0,N) \tag{3.13}$$

where

$$\omega=\frac{1}{2}\frac{(\kappa S_0)^{\frac{2}{3}}}{(\kappa X_0)^{\frac{1}{2}}} \tag{3.14}$$

is the only parameter left in the problem. Condition (2.9) is rendered into

$$\vartheta(0,Y)=0\quad\text{if } -\infty<Y<0. \tag{3.15}$$

We have now arrived at a formulation of the problem which is independent of the velocity distribution. The velocity is incorporated in the independent variables and in ω.

A formal solution to the equations (3.9) and (3.10) subject to the as yet unknown initial profiles at $S=0$ and $X=0$ is

$$\vartheta(X,Y)=\frac{1}{2\pi^{\frac{1}{2}}X^{\frac{1}{2}}}\int_0^\infty \vartheta(0,P)\mathrm{e}^{-\frac{(P-Y)^2}{4X}}dP, \tag{3.16}$$

$$\theta(S,N)=\frac{\Gamma\left(\frac{1}{3},\frac{N^3}{9S}\right)}{\Gamma(\frac{1}{3})}+\frac{1}{3S}\int_0^\infty N^{\frac{1}{2}}P^{\frac{1}{2}}\mathrm{e}^{-\frac{N^3+P^3}{9S}}I_{\frac{1}{3}}\left(\frac{2}{9}\frac{N^{\frac{3}{2}}P^{\frac{3}{2}}}{S}\right)\theta(0,P)dP, \tag{3.17}$$

where $\Gamma(a,b)=\int_b^\infty t^{a-1}\mathrm{e}^{-t}dt$ is the incomplete Gamma function and $I_{\frac{1}{3}}(P)$ is a modified Bessel function. In deriving (3.16) the boundary condition (3.15) has been used. If we apply now the conditions of equation (3.13) we obtain a system of two integral equations for the unknown profiles $\theta(0,N)$ and $\theta(1,N)$:

$$\theta(0,N)=\frac{\omega}{\pi^{\frac{1}{2}}}\int_0^\infty P\mathrm{e}^{-\frac{\omega^2}{4}(P^2-N^2)^2}\theta(1,P)dP, \tag{3.18}$$

$$\theta(1, N) = \frac{\Gamma\left(\frac{1}{3}, \frac{N^3}{9}\right)}{\Gamma(\frac{1}{3})} + \tfrac{1}{3}\int_0^\infty N^{\frac{1}{2}} P^{\frac{3}{2}} e^{-\frac{N^3+P^3}{9}} I_{\frac{1}{3}}(\tfrac{2}{9} N^{\frac{3}{2}} P^{\frac{3}{2}}) \theta(0, P) dP. \tag{3.19}$$

It does not seem possible to find analytical solutions to these equations, but it is a rather simple matter to find numerical ones. In the method applied by us, we divide the region of integration into two separate intervals: a finite interval $[0, P_m]$ and an infinite $[P_m, \infty]$. At $P = P_m$ the profiles are assumed to have attained the (as yet unknown) asymptotic values. The finite interval is further divided into a great many subintervals. We then introduce two vectors, the entries of which are the unknown values of $\theta(0, N)$ and $\theta(1, N)$ at the vertices of these intervals. The integral over the interval $[0, P_m]$ is then reduced to a sum of integrals over each of the subintervals, where the intermediate values of $\theta(0, N)$ and $\theta(1, N)$ are found by linear interpolation. It is essential that we should not use a pointwise representation of the kernels of the integral equations. Indeed, these kernels can vary rather rapidly, even on subintervals. This is why an accurate calculation of subintegrals is required.

The integrals over the interval $[P_m, \infty]$ can be carried out at once, and these are either proportional to $\theta(0, P_m)$ or to $\theta(1, P_m)$. The problem is now reduced to the solution of linear algebraic equations and this solution can be found without much further ado.

Some temperature profiles inside the cavity are given in Figs. 2–4, whereas Fig. 5 displays profiles in the mixing region. It is seen that there is a rather strong dependence upon the parameter ω. It is found that for ω large the heat loss incurred in the mixing region is rapidly compensated for inside the cavity. At $S = 0.1$ the temperature profile does not differ very much from that at $S = 1$. On the other hand, for $\omega = 0.1$ there is still a long way to go at $S = 0.1$.

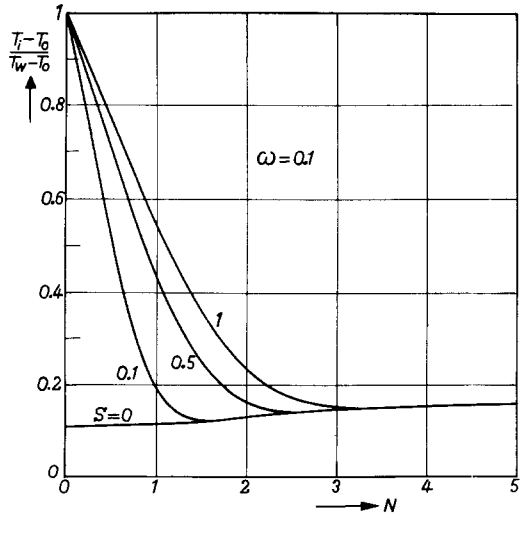

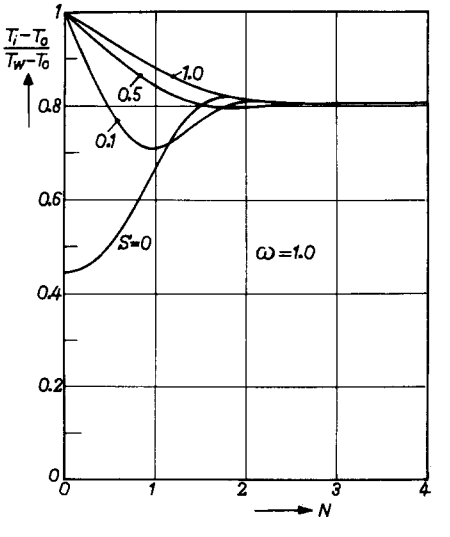

Figure 2. Temperature profiles in wall boundary layer ($\omega = 0.1$).

Figure 3. Temperature profiles in wall boundary layer ($\omega = 1.0$).

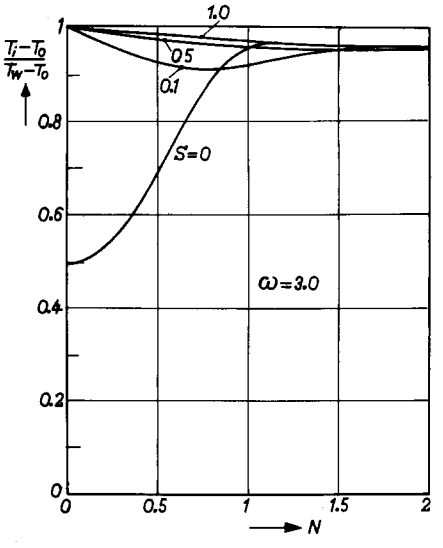

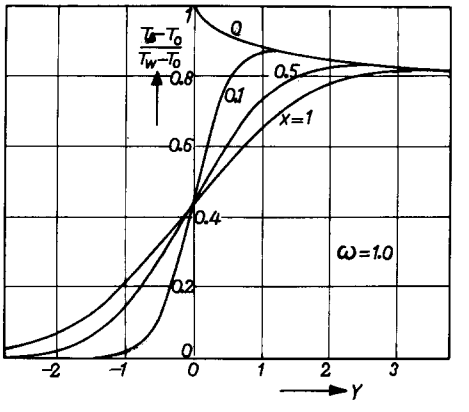

Figure 4. Temperature profiles in wall boundary layer ($\omega = 3.0$).

Figure 5. Temperature profiles in free boundary layer ($\omega = 1.0$).

The asymptotic temperature profile is also strongly dependent upon ω. This is shown clearly by Fig. 6, where we show the temperature in the core. Apparently, for $\omega \gg 1$, the cavity is almost closed, since the temperature is distributed almost uniformly throughout the cavity. The smallness of the orifice is the limiting factor in the heat transfer process. For a given orifice, a given velocity distribution at the orifice and a given temperature difference, there is a limit to the amount of heat that can leave the cavity and this will be reached for $\omega \to \infty$.

For $\omega \to 0$, it is the relative shortness of the cavity wall which is the limiting factor. Again, for given conditions near the wall there is a limit to the amount of heat that can leave the

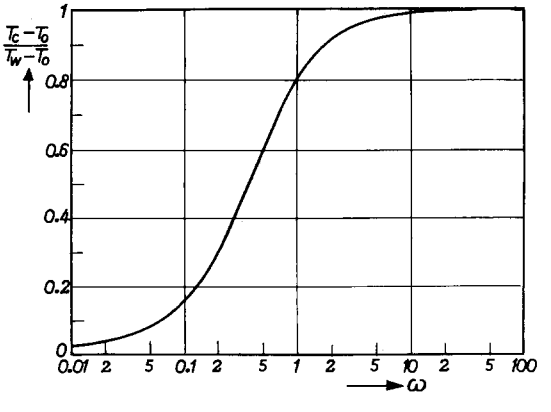

Figure 6. Temperature in the core as a function of ω.

wall and this is reached if $\omega = 0$. Then the cavity is as open as is possible. It should be emphasized that the terms "open" and "closed" are not meant to be solely geometrical. The terminology is based upon the parameter ω and thus it involves the velocity distribution and the thermal diffusivity of the particular fluid in addition to the actual geometry of the cavity.

The local heat transfer at the cavity wall is

$$q_w = -k \left. \frac{\partial T_i}{\partial n} \right|_{n=0}$$

where k is the thermal conductivity. Using the transformation formulae (3.5)–(3.8) we easily find from (3.17)

$$\frac{q_w(\kappa S_0)^{\frac{1}{3}}}{k(T_w - T_0)} \alpha(s)^{-\frac{1}{2}} = g(\omega, S)$$
$$= \frac{3^{\frac{1}{3}}}{\Gamma(\frac{1}{3})} S^{-\frac{1}{3}} - \frac{3^{-\frac{2}{3}}}{\Gamma(\frac{1}{3})} S^{-\frac{4}{3}} \int_0^\infty P^2 e^{-\frac{P^3}{9S}} \theta(0, P) dP. \tag{3.20}$$

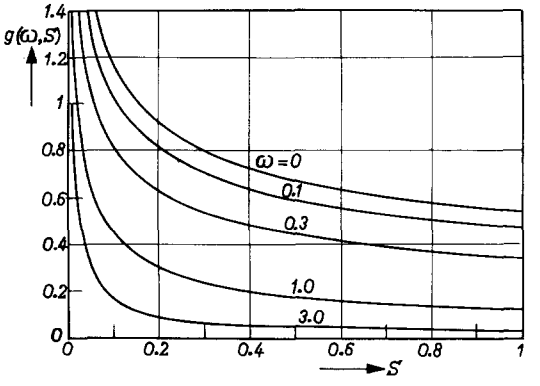

Figure 7. Local-heat-transfer function defined by Eq. (3.20).

The function $g(\omega, S)$ has been sketched in Fig. 7 for various values of ω and S. When interpreting these graphs we ought to keep in mind that the true S-dependence of q_w is given by the function $\alpha(s)^{\frac{1}{2}} g(\omega, S)$. This means that, as expected, heat transfer is large when the normal derivative of the longitudinal velocity component is large. Therefore, heat-flux profiles such as have been found by Burggraf [7] can be understood in the light of the present analysis.

For etching problems the local mass-transfer rate is of primary importance. We therefore present a detailed tabulation of the function $g(\omega, S)$ in Tables 1 and 2. For $S \to 0$ the function g becomes singular. Its behaviour can be obtained from Eq. (3.20) and is found to be

$$g(\omega, S) \sim \frac{3^{\frac{1}{3}}}{\Gamma(\frac{1}{3})} \{1 - \theta(0, 0)\} S^{-\frac{1}{3}}. \tag{3.21}$$

TABLE 1
The function $g(\omega, S)$.

ω \ S	0.01	0.02	0.03	0.04	0.06	0.08	0.10	0.12	0.16
0.0	2.4988	1.9833	1.7326	1.5742	1.3752	1.2494	1.1599	1.0915	0.9917
0.1	2.2191	1.7603	1.5369	1.3957	1.2183	1.1063	1.0264	0.9654	0.8763
0.2	1.9873	1.5734	1.3714	1.2436	1.0829	0.9813	0.9087	0.8533	0.7721
0.3	1.8068	1.4258	1.2393	1.1210	0.9720	0.8776	0.8101	0.7584	0.6826
0.4	1.6690	1.3111	1.1354	1.0236	0.8825	0.7929	0.7287	0.6795	0.6072
0.6	1.4811	1.1505	0.9866	0.8819	0.7492	0.6647	0.6041	0.5577	0.4900
0.8	1.3624	1.0442	0.8854	0.7835	0.6542	0.5721	0.5135	0.4688	0.4043
1.0	1.2802	0.9672	0.8101	0.7092	0.5815	0.5009	0.4439	0.4009	0.3397
1.2	1.2183	0.9069	0.7501	0.6494	0.5228	0.4437	0.3885	0.3473	0.2897
1.5	1.1466	0.8343	0.6770	0.5767	0.4520	0.3758	0.3236	0.2855	0.2335
2.0	1.0556	0.7395	0.5818	0.4830	0.3637	0.2936	0.2474	0.2145	0.1711
2.5	0.9796	0.6626	0.5069	0.4114	0.2998	0.2366	0.1961	0.1680	0.1318
3.0	0.9152	0.5976	0.4454	0.3544	0.2512	0.1948	0.1595	0.1354	0.1049
4.0	0.8041	0.4924	0.3513	0.2709	0.1824	0.1393	0.1122	0.0942	0.0719
6.0	0.6304	0.3489	0.2344	0.1736	0.1124	0.0828	0.0656	0.0545	0.0411
8.0	0.5035	0.2596	0.1680	0.1215	0.0766	0.0557	0.0439	0.0363	0.0273
10.0	0.4100	0.2011	0.1269	0.0903	0.0559	0.0404	0.0317	0.0263	0.0198

TABLE 2
The function $g(\omega, S)$

ω \ S	0.2	0.3	0.4	0.5	0.6	0.7	0.8	0.9	1.0
0.0	0.9206	0.8042	0.7307	0.6783	0.6383	0.6063	0.5799	0.5576	0.5384
0.1	0.8128	0.7087	0.6428	0.5958	0.5599	0.5311	0.5074	0.4873	0.4700
0.2	0.7141	0.6188	0.5584	0.5153	0.4824	0.4561	0.4345	0.4162	0.4004
0.3	0.6284	0.5392	0.4829	0.4428	0.4125	0.3883	0.3686	0.3520	0.3378
0.4	0.5556	0.4710	0.4179	0.3807	0.3526	0.3306	0.3127	0.2978	0.2852
0.6	0.4419	0.3646	0.3176	0.2855	0.2619	0.2438	0.2293	0.2175	0.2075
0.8	0.3593	0.2889	0.2476	0.2202	0.2005	0.1856	0.1738	0.1643	0.1564
1.0	0.2979	0.2343	0.1982	0.1747	0.1583	0.1459	0.1363	0.1285	0.1222
1.2	0.2511	0.1939	0.1624	0.1423	0.1283	0.1180	0.1099	0.1035	0.0983
1.5	0.1995	0.1508	0.1249	0.1087	0.0976	0.0894	0.0831	0.0782	0.0741
2.0	0.1439	0.1062	0.0868	0.0750	0.0670	0.0612	0.0568	0.0533	0.0504
2.5	0.1095	0.0796	0.0646	0.0556	0.0496	0.0453	0.0420	0.0394	0.0373
3.0	0.0866	0.0623	0.0503	0.0432	0.0384	0.0350	0.0325	0.0304	0.0288
4.0	0.0588	0.0418	0.0336	0.0287	0.0255	0.0232	0.0215	0.0201	0.0190
6.0	0.0334	0.0235	0.0188	0.0160	0.0142	0.0129	0.0119	0.0111	0.0105
8.0	0.0222	0.0156	0.0125	0.0106	0.0094	0.0085	0.0079	0.0073	0.0069
10.0	0.0161	0.0113	0.0090	0.0077	0.0068	0.0061	0.0057	0.0053	0.0050

Here it should be emphasized that $\theta(0, 0)$ refers to the initial profile which is obtained from (3.13). The value of $\theta(0, 0)$ is given in Table 3. For very small and very large values of ω the information of the tables will be supplemented by asymptotic results to be obtained in the following sections.

TABLE 3
The constant occurring in Eq. (3.21) *for various values of* ω.

ω	0.05	0.1	0.2	0.3	0.4	0.6	0.8	1.0
$\theta(0, 0)$	0.0578	0.1111	0.2014	0.2699	0.3205	0.3855	0.4222	0.4444
ω	1.5	2.0	3.0	4.0	6.0	8.0	10.0	
$\theta(0, 0)$	0.4716	0.4830	0.4921	0.4955	0.4980	0.4988	0.4993	

The total heat transfer Q_w from the cavity is of particular interest. Since we have

$$Q_w = \int_0^{s_0} q_w(s)ds$$

we can easily derive from (3.20), using the transformations (3.5)–(3.8)

$$\frac{Q_w\{(KS_0)^{-\frac{2}{3}} + (KX_0)^{-\frac{1}{2}}\}}{\rho c_p(T_w - T_0)} = f(\omega) =$$

$$= (1 + 2\omega)\left\{\frac{3^{\frac{4}{3}}}{2\Gamma(\frac{1}{3})} - \frac{1}{\Gamma(\frac{1}{3})}\int_0^{\infty} P\theta(0, P)\Gamma\left(\frac{1}{3}, \frac{P^3}{9}\right)dP\right\}. \tag{3.22}$$

The function $f(\omega)$ is shown in Fig. 8. A careful examination of (3.21) and Fig. 8 shows again that for $\omega \to \infty$ it is the phenomena at the orifice that set a limit to heat transfer, whereas for $\omega \to 0$ it is those at the cavity wall. To explain this we consider the relative magnitude of the terms $(\kappa S_0)^{-\frac{2}{3}}$ and $(\kappa X_0)^{-\frac{1}{2}}$ and the fact that $f(\omega)$ is of order unity and boundedly away from zero.

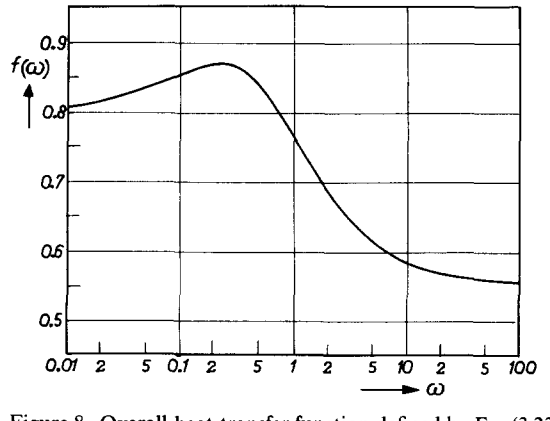

Figure 8. Overall-heat-transfer function defined by Eq. (3.22).

4. The case $\omega \ll 1$

It will be of interest to present a more detailed description of the solution valid for $\omega \to 0$. To do this we shall start from the differential equations and boundary conditions (3.9)–(3.15). The condition (3.13) is of special interest. Suppose that for $\omega \to 0$ the variable Y remains the natural variable measuring the width of the free boundary layer in the mixing region. Then we see from (3.13) that the width of the initial profile $\theta(0, N)$ cannot be measured by variations of N that are of order unity. The natural boundary-layer variable in the vicinity of the cavity wall seems to be

$$\tilde{N} = N\omega^{\frac{1}{2}} \tag{4.1}$$

which we shall call the outer variable. Introducing the outer temperature

$$\tilde{\theta}(S, \tilde{N}) = \theta(S, \tilde{N}\omega^{-\frac{1}{2}}) \tag{4.2}$$

we may transform the differential equation of (3.10) into

$$\frac{\partial \tilde{\theta}}{\partial S} = \omega^{\frac{1}{2}} \tilde{N}^{-1} \frac{\partial^2 \tilde{\theta}}{\partial \tilde{N}^2}. \tag{4.3}$$

It is easy to see that this equation is satisfied by the following asymptotic expansion

$$\tilde{\theta}(S, \tilde{N}) = \sum_{m=0}^{m_1} \frac{\omega^{\frac{3m}{2}} S^m}{m!} \left(\tilde{N}^{-1} \frac{\partial^2}{\partial \tilde{N}^2}\right)^m \vartheta(1, \tilde{N}^2) + O\{\omega^{\frac{3(m_1+1)}{2}}\} \tag{4.4}$$

For $S \to 0$ this expansion satisfies the requisite condition given by (3.13). It is obvious that the condition at infinity, given by (3.10), is satisfied by (4.4) if $\vartheta(1, Y)$ tends to a constant when $Y \to \infty$. For $\tilde{N} \downarrow 0$, however, the expansion (4.4) can by no means yield the proper value $\tilde{\theta} = 1$. We shall have to introduce an inner layer near the cavity wall in which diffsion and convection are in balance. Since the two terms of the equation (3.10) are to be of equal importance, it follows that N is the natural inner variable. Introducing the inner temperature

$$\hat{\theta}(S, N) = \theta(S, N) \tag{4.5}$$

and expanding the second of the conditions given by (3.13) for small values of ω, we are led to introduce an inner expansion

$$\hat{\theta} = \sum_{m=0}^{m_2} \omega^m \hat{\theta}_m(S, N). \tag{4.6}$$

Each of the expansion functions satisfies the differential equation (3.10). At $N = 0$ we have

$$\hat{\theta}_m = \begin{cases} 1, & m = 0 \\ 0, & m \neq 0 \end{cases} \tag{4.7}$$

while at $S = 0$ we have

$$\hat{\theta}_m(0, N) = \frac{N^{2m}}{m!}\vartheta^{(m)}(1, 0) \tag{4.8}$$

where $\vartheta^{(m)}$ stands for the m^{th} derivative of ϑ with respect to the second argument. It may be emphasized that the derivatives of ϑ in (4.4) and (4.8) are still functions of ω. If the problem had been non-linear we should have had to do the analysis on a term-by-term basis, determining unknown terms as we go along. However, now that the problem is linear we may concentrate on the N-dependence of the solution and establish the full ω-dependence in the process.

Omitting details, we obtain the solution

$$\hat{\theta} = \frac{\Gamma\left(\frac{1}{3}, \frac{N^3}{9S}\right)}{\Gamma(\frac{1}{3})} + \sum_{m=0}^{m_2} \frac{3^{\frac{4m-2}{3}}\Gamma(\frac{3}{2}m + 1)}{\Gamma(\frac{4}{3})m!} \times$$

$$\times\, \omega^m \vartheta^{(m)}(1, 0) N S^{\frac{2m-1}{3}} M\left(\frac{1-2m}{3}, \frac{4}{3}, -\frac{N^3}{9S}\right) + O(\omega^{m_2+1}) \tag{4.9}$$

where $M(a, b, z)$ is the Confluent Hypergeometric function that admits the expansion

$$M(a, b, z) = \sum_{m=0}^{\infty} \frac{(a)_m}{(b)_m} \frac{z^m}{m!}$$

where

$$(a)_m = a(a-1)(a-2)\ldots(a-m+1), \quad (a)_0 = 1.$$

A generally valid solution is obtained by the expression

$$\theta = \hat{\theta} + \tilde{\theta} - CP \tag{4.10}$$

where CP is the common part of $\hat{\theta}$ and $\tilde{\theta}$. As is well known, this common part can be derived by evaluating (4.4) for small values of $\tilde{N}$ and by evaluating (4.9) for $N \gg 1$. The common part of the resulting two expressions is the common part of the expansions (4.4) and (4.9). We find

$$CP = \sum_{i=0}^{m_2} \frac{N^{2i}\omega^i \vartheta^{(i)}(1, 0)}{i!} \sum_{m=0}^{m_1} \frac{\left(\frac{2i}{3}\right)_m \left(\frac{2i-1}{3}\right)_m}{m!} \left(\frac{9S}{N^3}\right)^m. \tag{4.11}$$

The heat-transfer problem near the cavity wall has now been solved formally for a given initial temperature profile. But of course the temperature profile at the entrance of the cavity is unknown. We have to complete the circle by writing (4.10) at $S = 1$, translating the resulting expression into an initial condition for the free boundary layer by making use of the first condition of (3.13) and solving the equation for the free boundary layer. In order not

to make things unduly complicated we shall only use two-term expansions for $\hat{\theta}$ and $\tilde{\theta}$, i.e. $m_1 = m_2 = 1$. From the general solution for the free boundary layer (3.16) we then see that the temperature profile $\vartheta(1, Y)$ must satisfy the equation

$$\vartheta(1, Y) = \mathscr{L}_1\{\vartheta(1, Y)\} + \omega \frac{1 - \vartheta(1,0)}{2\pi^{\frac{1}{2}}\Gamma(\frac{1}{3})} \int_0^\infty \Gamma\left(\frac{1}{3}, \frac{P^{\frac{3}{2}}}{9}\right) e^{-\frac{(Y-\omega P)^2}{4}} dP +$$
$$+ \frac{\omega^{\frac{3}{2}}}{\pi^{\frac{1}{2}}} \int_0^\infty \{P^{-\frac{1}{2}}\vartheta^{(1)}(1, P) + 2P^{\frac{1}{2}}\vartheta^{(2)}(1, P)\} e^{-\frac{(P-Y)^2}{4}} dP +$$
$$+ \frac{\omega^2 \vartheta^{(1)}(1,0)}{\pi^{\frac{1}{2}}} \int_0^\infty e^{-\frac{(Y-\omega P^2)^2}{4}} \left\{ \frac{2\Gamma(\frac{2}{3})3^{\frac{1}{2}}}{\Gamma(\frac{1}{3})} P^2 M\left(-\frac{1}{3}, \frac{4}{3}, -\frac{P^3}{9}\right) - P^3 - 2 \right\} dP +$$
$$+ \text{higher orders of } \omega, \tag{4.12}$$

where

$$\mathscr{L}_1\{G(Y)\} = \frac{1}{2\pi^{\frac{1}{2}}} \int_0^\infty e^{-\frac{(Y-P)^2}{4}} G(P) dP. \tag{4.13}$$

For small values of ω we have

$$\int_0^\infty \Gamma\left(\frac{1}{3}, \frac{P^{\frac{3}{2}}}{9}\right) e^{-\frac{(Y-\omega P)^2}{4}} dP \sim$$
$$\sim e^{-\frac{Y^2}{4}} \left\{ 3^{\frac{1}{2}} + \frac{3^{\frac{1}{2}}\Gamma(\frac{2}{3})}{2} Y\omega + 3\Gamma(\tfrac{1}{3})(Y^2 - 1)\omega^2 + O(\omega^3) \right\}. \tag{4.14}$$

Although this expansion is not uniformly valid on the interval $[0, \infty)$ it can be used with success if ω is small enough. The reason is that the incomplete Gamma function behaves exponentially if the argument tends to infinity. This means that for $\omega \ll 1$ the corrections to (4.14) are exponentially small. The same cannot be said of the integral involving the Confluent Hypergeometric function. This function behaves algebraically for large values of the argument. However, the leading term of an expansion of this integral valid for $\omega \to 0$ can de obtained by simply putting $\omega = 0$ under the integral sign.

We can now solve equation (4.12) by substituting the series

$$\vartheta(1, Y) = \omega F_1(Y) + \omega^2 F_2(Y) + \omega^{\frac{3}{2}} F_3(Y) + \omega^3 F_4(Y) + o(\omega^3) \tag{4.15}$$

where the F_i satisfy the equations

$$F_1(Y) = \mathscr{L}_1(F_1) + \frac{3^{\frac{1}{2}}}{2\pi^{\frac{1}{2}}\Gamma(\frac{1}{3})} e^{-\frac{Y^2}{4}}, \tag{4.16}$$

$$F_2(Y) = \mathscr{L}_1(F_2) + \frac{3^{\frac{1}{2}}\Gamma(\frac{2}{3})}{4\pi^{\frac{1}{2}}\Gamma(\frac{1}{3})} Y e^{-\frac{Y^2}{4}} - \frac{3^{\frac{1}{2}}}{2\pi^{\frac{1}{2}}\Gamma(\frac{1}{3})} F_1(0) e^{-\frac{Y^2}{4}}, \tag{4.17}$$

$$F_3(Y) = \mathscr{L}_1(F_3) + \frac{1}{\pi^{\frac{1}{2}}} \int_0^\infty \{P^{-\frac{1}{2}}F_1'(P) + 2P^{\frac{1}{2}}F_1''(P)\} e^{-\frac{(Y-P)^2}{4}} dP, \tag{4.18}$$

$$F_4(Y) = \mathscr{L}_1(F_4) + \frac{3}{2\pi^{\frac{1}{2}}}(Y^2-1)e^{-\frac{Y^2}{4}} - \frac{3^{\frac{4}{3}}\Gamma(\frac{2}{3})}{4\pi^{\frac{1}{2}}\Gamma(\frac{1}{3})}F_1(0)\,Ye^{-\frac{Y^2}{4}} -$$

$$- \frac{3^{\frac{4}{3}}}{2\pi^{\frac{1}{2}}\Gamma(\frac{1}{3})}F_2(0)e^{-\frac{Y^2}{4}} - \frac{3^{\frac{4}{3}}}{2\pi^{\frac{1}{2}}}\frac{\Gamma(\frac{2}{3})}{\Gamma(\frac{1}{3})}F_1'(0)e^{-\frac{Y^2}{4}}. \tag{4.19}$$

These are integral equations of the Wiener–Hopf type. Eq. (4.16) in particular was considered by Stewartson [14], but his analysis is very complicated. We have therefore solved these equations numerically, which can be done in a straightforward manner if we apply the technique described earlier in this paper.

Once the asymptotic expansion for $\vartheta(1, Y)$ is known, we are in a position to derive all the relevant results for $\omega \to 0$. The non-dimensional temperature in the core of the cavity is obtained by the calculation of $\theta(1, \infty)$. We find

$$\vartheta_c = 1.6151\omega + 0.4021\omega^2 - 1.156\omega^{\frac{4}{3}} + 3.013\omega^3 + o(\omega^3). \tag{4.20}$$

For the function $g(\omega, S)$, which according to (3.20) characterizes local heat transfer at the cavity wall, we get an explicit expression

$$g(\omega, S) = 0.53836S^{-\frac{1}{3}} - 0.64076S^{-\frac{1}{3}}\omega +$$

$$+ (0.30156S^{-\frac{1}{3}} - 0.92219S^{\frac{1}{3}})\omega^2 + 0.101\omega^{\frac{4}{3}}S^{-\frac{1}{3}} +$$

$$+ (0.33995S^{-\frac{1}{3}} - 1.0422S^{\frac{1}{3}} + 1.1872S)\omega^3 + o(\omega^3). \tag{4.21}$$

Finally, the overall heat-transfer function $f(\omega)$, which was introduced in Eq. (3.21), can be given as

$$f(\omega) = 0.80754 + 0.6539\omega - 2.1616\omega^2 + 0.1515\omega^{\frac{4}{3}} - 0.1567\omega^3 + o(\omega^3). \tag{4.22}$$

5. The case $\omega \gg 1$

At the other end of the ω-scale the solution can also be given in asymptotic form. We expect that now it will be the free boundary layer which reveals a double-layer character. If we write the first of the patching conditions (3.13) as

$$\vartheta(0, Y) = \theta(1, Y^{\frac{1}{2}}\omega^{-\frac{1}{2}}) \tag{5.1}$$

we find that the natural coordinate for the outer part of the free boundary layer is

$$\tilde{Y} = \omega^{-1}Y. \tag{5.2}$$

If we define an outer temperature

$$\tilde{\vartheta}(X, Y) = \vartheta(X, \omega\tilde{Y}) \tag{5.3}$$

we see that the equation resulting from (3.9) is satisfied by

$$\vartheta = \sum_{m=0}^{m_1} \frac{X^m \omega^{-2m}}{m!} \frac{\partial^{2m}}{\partial \tilde{Y}^{2m}} \theta(1, \tilde{Y}^{\frac{1}{2}}) + O(\omega^{-2m_1-2}). \tag{5.4}$$

It should be clear that this solution is only valid in the region $\tilde{Y} > 0$. Indeed, the validity of the patching condition (5.1) is restricted to that region. We must therefore search for a solution that is valid in the remaining part of the interval $-\infty < Y < \infty$. To do so we shall define an inner temperature

$$\hat{\vartheta}(X, Y) = \vartheta(X, Y) \tag{5.5}$$

Expanding (5.1) for large values of ω we see that the inner temperature satisfies the condition

$$\hat{\vartheta}(0, Y) = \sum_{m=0}^{m_2} \frac{\omega^{-\frac{m}{2}} Y^{\frac{m}{2}}}{m!} \theta^{(m)}(1, 0) + O(\omega^{-\frac{m_2+1}{2}}), \qquad (Y \geqslant 0) \tag{5.6}$$

where the superscript (m) denotes the m^{th} derivative with respect to the second argument. We also have

$$\hat{\vartheta}(0, Y) \equiv 0, \qquad (Y < 0). \tag{5.7}$$

Just as in the previous section, the function θ in (5.4) and (5.6) is still dependent on ω. Again, the linearity of the problem allows us to proceed without a detailed knowledge of this functional dependence. It would seem that the inner solution can be given as the asymptotic expansion

$$\hat{\vartheta} = \sum_{m=0}^{m_2} \frac{\omega^{-\frac{m}{2}} \theta^{(m)}(1, 0)}{m!} \hat{\vartheta}_m(X, Y) + O(\omega^{-\frac{m_2+1}{2}}). \tag{5.8}$$

Each of the expansion functions satisfies the system

$$\frac{\partial \vartheta_m}{\partial X} = \frac{\partial^2 \vartheta_m}{\partial Y^2}, \qquad \vartheta_m(0, Y) = \begin{cases} Y^{\frac{m}{2}} & (Y \geqslant 0) \\ 0 & (Y < 0) \end{cases} \tag{5.9}$$

It is not difficult to find the unique solution

$$\hat{\vartheta}_m = \frac{(4X)^{\frac{m}{4}}}{2\pi^{\frac{1}{2}}} \left\{ \Gamma\left(\frac{m}{4} + \frac{1}{2}\right) M\left(-\frac{m}{4}, \frac{1}{2}, -\frac{Y^2}{4X}\right) + \right.$$
$$\left. + \Gamma\left(\frac{m}{4} + 1\right) \frac{Y}{X^{\frac{1}{2}}} M\left(\frac{1}{2} - \frac{m}{4}, \frac{3}{2}, -\frac{Y^2}{4X}\right) \right\}. \tag{5.10}$$

For even values of m these functions are related to the error function, whereas for odd values of m the functions are related to parabolic cylinder functions. A generally valid solution can be obtained by adding the inner and outer solutions and subtracting the common part

$$\vartheta = \tilde{\vartheta} + \hat{\vartheta} - \sum_{m=0}^{m_2} \frac{\omega^{-\frac{m}{2}}\theta^{(m)}(1,0)Y^{\frac{m}{2}}}{m!} \sum_{r=0}^{m_1} \frac{\left(-\frac{m}{4}\right)_r \left(\frac{1}{2}-\frac{m}{4}\right)_r}{r!} \left(\frac{4X}{Y^2}\right)^r. \tag{5.11}$$

The next step is to determine the value of (5.11) at $X = 1$. Having done so, we are able to use the second of the patching conditions of Eq. (3.13) to derive an initial condition for the wall boundary layer. At this point the analysis becomes rather too complicated for a general exposition. This is why shall carry out the analysis using only two terms of the inner and two terms of the outer expansion, i.e. $m_1 = m_2 = 1$. The initial θ-profile is then

$$\begin{aligned}\theta(0,N) = \theta(1,N) &+ \theta(1,0)\left\{\tfrac{1}{2}\operatorname{erfc}\left(-\frac{\omega N^2}{2}\right) - 1\right\} + \\ &+ \omega^{-\frac{1}{2}}\theta^{(1)}(1,0)\left\{\frac{\Gamma(\frac{3}{4})}{(2\pi)^{\frac{1}{2}}} M\left(-\frac{1}{4},\frac{1}{2},-\frac{\omega^2N^4}{4}\right) + \right. \\ &\left. + \omega N^2 \frac{\Gamma(\frac{5}{4})}{(2\pi)^{\frac{1}{2}}} M\left(\frac{1}{4},\frac{3}{2},-\frac{\omega^2N^4}{4}\right) - \omega^{\frac{1}{2}}N\right\} + \\ &+ \omega^{-2}\{-\tfrac{1}{4}N^{-3}\theta^{(1)}(1,N) + \tfrac{1}{4}N^{-2}\theta^{(2)}(1,N) + \tfrac{1}{4}\theta^{(1)}(1,0)N^{-3}\}.\end{aligned} \tag{5.12}$$

In (5.12) we can substitute $\theta(1,0) = 1$ since this is the boundary condition (3.10). The role played by the terms of the common part is clear now. These terms offset the singularities of the outer expansion at $N = 0$ and they offset those terms of the inner expansion that become unbounded as $N \to \infty$.

The general solution for the wall boundary layer is given by (3.17). Using this equation for $S = 1$ and substituting Eq. (5.12) we obtain an integral equation for the unknown temperature profile $\theta(1, N)$:

$$\theta(1,N) = \frac{\Gamma\left(\frac{1}{3},\frac{N^3}{9}\right)}{\Gamma(\frac{1}{3})} + \mathscr{L}_2\{\theta(1,N)\} + \mathscr{L}_2\left\{\tfrac{1}{2}\operatorname{erfc}\left(-\frac{\omega N^2}{2}\right) - 1\right\} + \ldots \tag{5.13}$$

where

$$\mathscr{L}_2\{G(N)\} = \tfrac{1}{3}\int_0^\infty N^{\frac{1}{2}}P^{\frac{3}{2}}\mathrm{e}^{-\frac{N^3+P^3}{9}} I_{\frac{1}{3}}(\tfrac{2}{9}N^{\frac{3}{2}}P^{\frac{3}{2}})G(P)dP. \tag{5.14}$$

In Appendix A we obtain expansions for the integrals occurring in (5.13) that are valid for $\omega \to \infty$. Using these we can write (5.13) as follows

$$\begin{aligned}\theta(1,N) = \frac{\Gamma\left(\frac{1}{3},\frac{N^3}{9}\right)}{\Gamma(\frac{1}{3})} &+ \mathscr{L}_2\{\theta(1,N)\} - \frac{\Gamma(\frac{5}{4})}{3^{\frac{5}{3}}\Gamma(\frac{1}{3})}\left(\frac{2}{\pi}\right)^{\frac{1}{4}} N\mathrm{e}^{-\frac{N^3}{9}}\omega^{-\frac{3}{4}} + \\ &+ \frac{2}{3^{11/3}\Gamma(\frac{1}{3})\pi^{\frac{1}{2}}} N\left(1-\frac{N^3}{12}\right)\mathrm{e}^{-\frac{N^3}{9}}\omega^{-3} - \\ &- \frac{3^{\frac{1}{3}}}{24\Gamma(\frac{1}{3})} N\mathrm{e}^{-\frac{N^3}{9}}\theta^{(1)}(1,0)\omega^{-2}\ln\omega + O(\omega^{-\frac{7}{4}}).\end{aligned} \tag{5.15}$$

In (5.15) we have already anticipated that $\theta^{(1)}(1, 0) = O(\omega^{-\frac{1}{2}})$. Since we have

$$\mathscr{L}_2(1) = 1 - \frac{\Gamma\left(\frac{1}{3}, \frac{N^3}{9}\right)}{\Gamma(\frac{1}{3})} \tag{5.16}$$

we can solve (5.15) by putting

$$\theta(1, N) = 1 + G_1(N)\omega^{-\frac{1}{2}} + G_2(N)\omega^{-3} + G_3(N)\omega^{-\frac{7}{2}} \ln \omega + O(\omega^{-\frac{7}{2}}). \tag{5.17}$$

Up to the order considered the problem is now reduced to the solution of two integral equations of the type

$$\bar{G}_i(N) = \mathscr{L}_2\{\bar{G}_i(N)\} + N^i \mathrm{e}^{-\frac{N^3}{9}} \qquad (i = 1, 4) \tag{5.18}$$

and we have solved these equations numerically. We are now in a position to derive some important asymptotic results. We may obtain an expression for the core temperature by evaluating (5.17) for large values of N

$$\theta_c = 1 - 0.24108\omega^{-\frac{1}{2}} + 0.01947\omega^{-\frac{7}{2}} \ln \omega + O(\omega^{-\frac{7}{2}}). \tag{5.19}$$

We found numerically that the term which is proportional to ω^{-3} is cancelled in Eq. (5.19).

It is also a rather straightforward matter to derive an expression for the function $f(\omega)$, which was defined in Eq. (3.21) and which characterizes the total heat transfer from the cavity. Without going through the tedium of giving all the analytical details, we can state the following result

$$\begin{aligned} f(\omega) &= (1 + 2\omega)\left\{\frac{1}{2\pi^{\frac{1}{2}}}\omega^{-1} + \left(\frac{2}{\pi}\right)^{\frac{1}{2}} \frac{\Gamma(\frac{5}{4})}{\Gamma(\frac{1}{3})} G_1'(0)\omega^{-3} + \text{higher orders}\right\} \\ &= 0.5642 + 0.2821\omega^{-1} - 0.0848\omega^{-2} + \ldots \end{aligned} \tag{5.20}$$

To conclude this section we shall derive an asymptotic result for the local-heat-transfer function $g(\omega, S)$ defined by Eq. (3.20). From (5.12) and (5.17) it follows that we may write

$$\theta(0, P) \sim \tfrac{1}{2}\operatorname{erfc}\left(-\frac{\omega P^2}{2}\right) + \omega^{-\frac{1}{2}} G_1(P) + \text{higher orders} \tag{5.21}$$

and we can substitute this in (3.20). Omitting details of the analytical derivation we can state the following results. If

$$\gamma = \frac{2^{\frac{3}{2}}}{9S\omega^{\frac{1}{2}}} \ll 1 \tag{5.22}$$

then

$$g(\omega, S) = \omega^{-\frac{1}{2}} S^{-\frac{1}{4}}\left\{\frac{2^{\frac{1}{2}}\Gamma(\frac{5}{4})}{3^{\frac{1}{4}}\pi^{\frac{1}{4}}\Gamma(\frac{1}{3})} - \frac{3^{-\frac{1}{4}}}{\Gamma(\frac{1}{3})}\int_0^\infty P^2 \mathrm{e}^{-\frac{P^3}{9S}} G_1(P)\,dP\right\}. \tag{5.23}$$

This result is tabulated in Table 4. Obviously the local heat transfer behaves as $\omega^{-\frac{2}{3}}$ if ω tends to infinity.

TABLE 4

S	0	0.1	0.2	0.3	0.4	0.5	0.6	0.7	0.8	0.9	1.0
$g(\omega,S)\omega^{\frac{1}{3}}S^{\frac{1}{3}}$	0.0433	0.0502	0.0599	0.0707	0.0821	0.0940	0.1060	0.1183	0.1307	0.1432	0.1558

If γ is not very small, which can only be the case if $S \ll 1$, the asymptotic result is

$$g(\omega, S) \sim \frac{3^{\frac{1}{3}}}{\Gamma(\frac{1}{3})}\left\{\frac{1}{2} - \frac{1}{\pi^{\frac{1}{2}}}\int_0^\infty e^{-t^2-\gamma t^{\frac{1}{3}}}dt\right\}S^{-\frac{1}{3}}. \tag{5.24}$$

This result is tabulated in Table 5.

TABLE 5

γ	0.1	0.2	0.4	0.6	1.0	2.0	4.0	6.0	8.0	10.0
$g(\omega,S)S^{\frac{1}{3}}$	0.0131	0.0248	0.0451	0.0620	0.0885	0.1302	0.1708	0.1912	0.2036	0.2120

Finally, for $\gamma \gg 1$ the result (5.24) may be written asymptotically

$$g(\omega, S) \sim \frac{3^{\frac{1}{3}}}{2\Gamma(\frac{1}{3})} - \frac{2\cdot 3^{-\frac{1}{3}}}{\pi^{\frac{1}{2}}}\frac{\Gamma(\frac{2}{3})}{\Gamma(\frac{1}{3})}\gamma^{-\frac{1}{3}} + \frac{2\cdot 3^{-\frac{2}{3}}}{\pi^{\frac{1}{2}}\Gamma(\frac{1}{3})}\gamma^{-2} + O(\gamma^{-10/3}). \tag{5.25}$$

6. A few simple applications

A special feature of the present work is that the heat- or mass-transfer analysis can be formulated independently of the particular flow field. All the necessary information about the flow can be found in the dimensionless variables and the parameter ω. However, when it comes to applying our results we shall have to know the flow field in order to obtain the actual values of ω and the dimensional variables. In this chapter we shall apply our results to a few simple flows with closed streamlines. In order to keep the complication of the analysis within reasonable bounds, we shall use a prescribed velocity on the dividing streamline, i.e. we shall restrict ourselves to closed cavities.

The first example is that of a circular cavity with part of its circumference moving at a uniform azimuthal velocity u_0. If we use cylindrical coordinates (r, θ), with $-\pi < \theta < \pi$, the circumference will be at $r = r_0$ and its moving part is restricted to the interval $-\varphi/2 < \theta < \varphi/2$. If we assume a Reynolds number $u_0 r_0/\nu$ that is much less than unity, we can use the solution for the stream function ψ as it was given by Burggraf [7]

$$\frac{\psi}{u_0 r_0} = \frac{1-R^2}{2\pi}\left[\frac{\varphi}{2} + \arctan\left\{\frac{R\sin(\theta+\varphi/2)}{1-R\cos(\theta+\varphi/2)}\right\} - \right.$$
$$\left. - \arctan\left\{\frac{R\sin(\theta-\varphi/2)}{1-R\cos(\theta-\varphi/2)}\right\}\right] \tag{6.1}$$

where $R = r/r_0$. From this we may easily obtain the normal derivative of the azimuthal velocity at the non-moving part of the circumference ($|\theta| > \varphi/2$)

$$\tilde{\alpha} = \left.\frac{\partial^2\psi}{\partial r^2}\right|_{r=r_0} = \frac{u_0}{r_0}\frac{1}{\pi}\left[\operatorname{ctn}\left(\frac{2\theta-\varphi}{4}\right) - \operatorname{ctn}\left(\frac{2\theta+\varphi}{4}\right)\right]. \tag{6.2}$$

From (3.14) we can derive an expression for ω valid for the present case

$$\omega = \left(\frac{\kappa r_0}{4u_0^3\varphi^3}\right)^{\frac{1}{4}}\left(\int_{\varphi/2}^{\pi}\tilde{\alpha}^{\frac{1}{4}}d\theta\right)^{\frac{3}{4}}. \tag{6.3}$$

If we substitute (6.2) in (6.3) we find

$$\omega Pe^{\frac{1}{4}} = \left(\frac{2}{\pi}\right)^{\frac{1}{4}}\left(\frac{\sin\varphi/2}{\varphi}\right)^{\frac{1}{4}}\left\{\int_{\tan\varphi/2}^{\infty}(1+t^2)^{-1}\left(\cos\frac{\varphi}{2}+t\sin\frac{\varphi}{2}\right)^{-\frac{1}{4}}dt\right\}^{\frac{3}{4}} \tag{6.4}$$

with

$$Pe = \frac{u_0 r_0 \varphi}{\kappa}. \tag{6.5}$$

In (6.5) we have chosen $r_0\varphi$, the length of the moving part of the circumference, as the characteristic length. A graphical representation of the function (6.4) can be found in Fig. 9, where we have used for the abscissa the ratio of the length of the moving part and the total length of the circumference. It is clear that ω tends to zero if the Péclet number becomes larger. However, due to the smallness of the power to which the Péclet number is being raised in (6.4), we can still have values of ω that differ markedly from zero when Pe is only moderately large. Fig. 9 shows that this is particularly true if the moving part of the cavity boundary is relatively short.

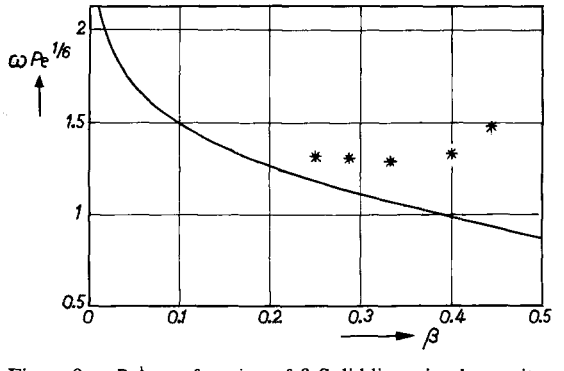

Figure 9. $\omega Pe^{\frac{1}{4}}$ as a function of β. Solid line: circular cavity; asterisks: rectangular cavity.

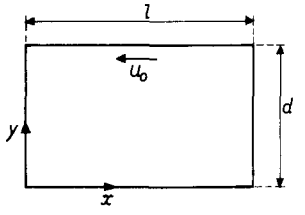

Figure 10. Geometry used for rectangular cavity.

As a second example we shall consider a rectangular cavity which has one of its sides moving with a velocity u_0 in a longitudinal direction. The geometry of the system is sketched in Fig. 10. If we again consider the case of creeping flow, i.e. if $u_0 l/\nu \ll 1$, the stream function ψ will satisfy the biharmonic equation. In terms of the non-dimensional quantities $\Psi = 2\psi/(u_0 l)$, $X = 2x/l$, $Y = 2y/l$, the flow is described by the following equation and boundary conditions

$$\Delta\Delta\Psi = 0 \tag{6.6}$$

$$\begin{aligned} &X = 0: && \Psi = 0,\ \Psi_X = 0,\\ &X = 1: && \Psi_X = 0 \text{ (line of symmetry)},\\ &Y = 0: && \Psi = 0,\ \Psi_Y = 0,\\ &Y = Y_0 = 2d/l: && \Psi = 0,\ \Psi_Y = -1. \end{aligned} \tag{6.7}$$

From (3.14) we may now easily derive the result

$$\omega Pe^{\frac{1}{3}} = \left\{\tfrac{1}{2}\int_0^{Y_0} (\Psi_{XX})_{X=0}^{\frac{1}{2}}\,dY + \tfrac{1}{2}\int_0^1 (\Psi_{YY})_{Y=0}^{\frac{1}{2}}\,dX\right\}^{\frac{2}{3}} \tag{6.8}$$

where

$$Pe = \frac{u_0 l}{\kappa}.$$

Quite a few authors have considered the problem defined by (6.6) and (6.7), e.g. Burggraf [7] and Pan and Acrivos [10], but they were mainly interested in the stream-line pattern. In any case, numerical values for the second derivatives of Ψ at the cavity wall cannot be obtained from the literature. This is why we had to solve the problem again and we decided to use the numerical software package ASKA, which employs finite elements. We did some runs for a few values of Y_0. Some of the results can be found in Fig. 11, where we display $\Psi_{YY}^{\frac{1}{2}}$ along the first half of the bottom wall of the cavity and $\Psi_{XX}^{\frac{1}{2}}$ along one of the side walls. In the neighbourhood of the corner, where both sides meet, the graphs have not been drawn since Ψ_{XX} and Ψ_{YY} change sign. Indeed, it has been known for some time (Moffatt [15]) that there exists an infinite sequence of eddies of ever diminishing strength in sharp corners. In terms of our heat-transfer model, described in section two, this means that the wall boundary layer is split up into two parts near every corner. The connection between the two parts is furnished

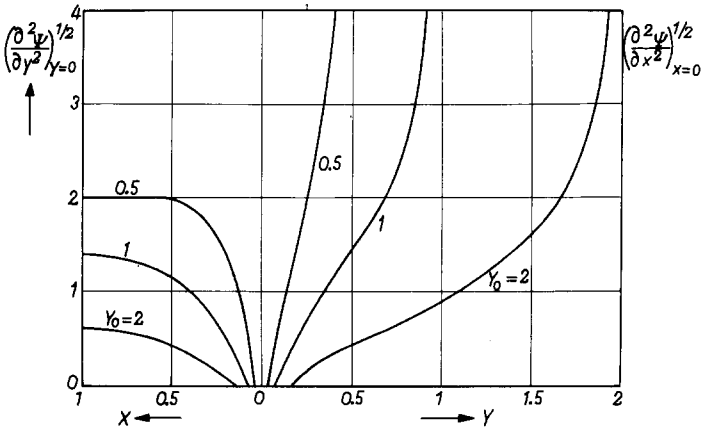

Figure 11. The local-heat-transfer function $\alpha^{\frac{1}{4}}$ at the wall of the rectangular cavity for various values of $Y_0 = 2d/l$.

by a free boundary layer along the dividing stream line in the corner. However, it appears from Fig. 11 that such a refined approach will but slightly improve the results. We shall therefore neglect the contribution of the corner and consider the wall boundary layer as continuous.

If we substitute our numerical results in Eq. (6.8) we obtain the results given by asterisks in Fig. 9. A further striking result is the fact that ω is virtually constant for a considerable range of aspect ratios. Since the overall heat transfer – or mass transfer in the case of etching – is a function of ω only, this result seems to confirm the observation reported by Goosen and Van Ruler [4] that the etching speed is constant in the initial stages of the etching process, i.e. as long as the single-cell approach is valid.

Since the integrand of the first integral of (6.8) becomes singular if $y \to y_0$, it will be necessary to employ an analytical representation of Ψ in the neighbourhood of $Y = Y_0$. It is not difficult to prove that the solution valid near the corner where the moving wall and the side wall meet, is given by

$$\Psi = \frac{\frac{\pi^2}{4}(Y_0 - Y) - \left\{X + \frac{\pi}{2}(Y_0 - Y)\right\} \arctan\left(\frac{Y_0 - Y}{X}\right)}{\frac{\pi^2}{4} - 1} \tag{6.9}$$

from which we may derive

$$(\Psi_{XX})^{\frac{1}{4}}_{X=0} = \left\{\frac{2}{(\pi^2/4 - 1)Y}\right\}^{\frac{1}{4}}. \tag{6.10}$$

The analytical solution (6.10) provides a good test for the accuracy of the computations done with ASKA.

The examples we have given both involve the assumption $Re \ll 1$. For large values of the Reynolds number, flows within cavities are usually more complicated. We shall therefore

confine ourselves to making some qualitative remarks on the application of our results to such flows. For $Re \gg 1$, Batchelor [9] has shown that the flow consists of an inviscid core of uniform vorticity. The no-slip condition at the wall demands the introduction of a viscous boundary layer. The longitudinal velocity u_c at the outer edge of the boundary layer can be calculated from the state of uniform vorticity in the core. If l is a characteristic length along the cavity wall we find

$$\alpha = O\left(\frac{u_c^3}{\nu l}\right). \tag{6.11}$$

If a part of the cavity wall of length δl moves at a velocity u_0, we find

$$\omega \sim Pr^{-\frac{1}{2}}\left(\frac{u_c}{u_0 \delta}\right)^{\frac{1}{2}} \tag{6.12}$$

where

$$Pr = \frac{\nu}{\kappa} \tag{6.13}$$

is the Prandtl number. For the cylindrical cavity introduced earlier Batchelor [9] gives the result $u_c = u_0 \delta^{\frac{1}{2}}$, which yields

$$\omega \sim Pr^{-\frac{1}{2}} \delta^{-\frac{1}{2}}. \tag{6.14}$$

7. Discussion of the results

In this paper we have made an attempt to devise a mathematical model for heat or mass transfer from cavity flows. The model is valid when both the Péclet number, based on cavity dimensions, and the Prandtl number are large. Despite these restrictions we expect that the model can be applied to a variety of situations. Indeed, in bio-fluid mechanics most fluids do have a large Prandtl number. The large Prandtl number condition is also met by etching fluids and lubrication oils. Due to the extremely low diflusivities of most of these fluids, the large-Pe condition will be violated only if flow velocities and cavity dimensions are exceedingly small. Goosen and Van Ruler [4], for example, use etching fluids with diflusivities as low as 10^{-9} m^2/s. Thus, for cavity dimensions as small as 10^{-5} m and flow velocities of 10^{-1} m/s, the Péclet number is still of the order of one thousand.

At its present stage of development the model cannot be applied to gases, the reason being that for most gases $Pr \sim 1$. The complication of the model will increase considerably if its range of applicability is to include gases. Indeed, for $Pr \sim 1$ the convection terms can no longer be simplified in the manner of section two. At this moment it is not clear if the simple analysis given in section three, involving integral equations, can be done if $Pr \sim 1$.

Since much of the work on heat transfer from open cavities has been done for air (e.g. Miles [5], Haugen and Dhanak [16], Fox [17]) a comparison with previous work can only be qualitative. Haugen and Dhanak did experiments on turbulent flows over open cavities. The temperature profiles measured by them do support the boundary-layer assumption

used by us. Their measurements reveal a virtually isothermal core and near the orifice and the bottom of the cavity they find temperature profiles which are clearly of a boundary-layer nature. It is interesting to note that for deeper cavities these authors measured temperature profiles that can be explained by the multiple boundary-layer model which applies when there is more than one vortex. We put forward this idea in the introduction to explain a sudden drop in etching speed. The temperature profiles measured by Haugen et al. for deeper cavities show that the temperature rises again in the lower part of the cavity after having been constant over most of the upper vortex.

In the introduction we mentioned thrombogenesis as a possible application of the present work. Benis et al. [18] did some experimental work in this field. They studied thrombus formation in a cavity introduced in an extracorporeal shunt joining the carotid artery and the jugular vein of a dog. From Fig. 2 of their paper we may conclude that thrombus formation is inversely proportional to the square root of the Reynolds number. This result may be explained by our analysis if we assume that ω was large in the experiments performed by Benis et al. Indeed, from (3.22) we may then conclude that mass transfer from the cavity increases proportionally to $X_0^{\frac{1}{2}}$. We may expect that larger mass-transfer rates will slow down the growth of a thrombus.

From a paper by C. G. Caro, J. M. Fitz-Gerald and R. C. Schroter [19] it appears that some forms of early atheroma may be explained along the same lines as thrombogenesis. Atheroma is a degeneration of the arterial wall which leads to hardening of the arteries. It is thought that cholesterol synthesized within the blood stream is instrumental in thin degenerative process. Caro et al. discovered that this phenomenon was to be found in regions of low wall shear stress. It was particularly conspicuous in regions of separated blood flow that are to be found directly downstream of junctions of large arteries. These authors put the Schmidt number associated with cholesterol diffusion at about 10^5. Also, in large arteries the Reynolds number is $\approx 10^2$–10^3, so that $ReSc \gg 1$. This shows that our cavity model may be applied to describe diffusion of cholesterol in regions of separated blood flow and to give a quantitative account of incipient atheroma.

To conclude we shall discuss possible extensions of the present work. An important generalization will be the two-cell model referred to earlier and which applies to cavities of depth-width ratios roughly between one and two. This case will feature two free boundary layers, one near the orifice of the cavity and one along the streamline dividing the two cells. There will be three separate wall boundary layers now, two of which will join the ends of the free boundary layers along the rim of the upper vortex. The third of the wall boundary layers will be along the remaining part of the lower cell. Mathematically the solution will be governed by a set of five coupled integral equations and it is likely that more than one parameter such as ω will influence the problem. Extensions to more cells are easily envisaged but clearly the numerical complication will increase correspondingly. A somewhat simpler extension applies when the free stream follows the cavity wall part of the way down before separation occurs. In that case there will be a wall boundary layer along that portion of the cavity wall that produces a non-uniform temperature or concentration profile at the point of separation where the free boundary layer emerges. The analysis of this paper applies almost unaltered to this situation. The only change will be in the boundary condition (2.9), where now the effect of the above-mentioned wall boundary layer will be felt.

Acknowledgement

The author is indebted to Dr. C. Weber of Philips Research Laboratories for his assistance in the application of the finite-element package ASKA.

Nomenclature (most important symbols only)

c: heat capacity
f: dimensionsless function related to total heat transfer (3.22)
g: dimensionless function related to local heat transfer (3.20)
k: thermal conductivity
l: characteristic length
n: dimensional coordinate measuring distance from cavity wall
N: dimensionless coordinate measuring distance from cavity wall
Pe: Péclet number: $u_0 l/\kappa$
Pr: Prandtl number: ν/κ
q_w: local heat transfer
Q_w: total heat transfer
Re: Reynolds number: $u_0 l/\nu$
s: dimensional coordinate measuring distance along cavity wall
s_0: length of cavity wall
S: dimensionless coordinate measuring distance along cavity wall
S_0: parameter defined by (3.8)
T: temperature in free boundary layer
T_0: temperature of the surrounding fluid
T_c: temperature in the core
T_i: temperature in the wall boundary layer
T_w: temperature of the cavity wall
u: longitudinal velocity in free boundary layer
u_0: characteristic velocity in free boundary layer
x: dimensional coordinate measuring distance along free boundary layer
x_0: length of free boundary layer
X: dimensionless coordinate measuring distance along free boundary layer
X_0: parameter defined by (3.4)
y: dimensional coordinate measuring distance from dividing stream line
Y: dimensionless coordinate measuring distance from dividing stream line
α: normal derivative of longitudinal velocity at cavity wall
β: relative length of free boundary layer
δ_n: thickness of wall boundary layer
δ_y: thickness of free boundary layer
κ: thermal diffusivity: $k/\rho/c$
ν: kinematic viscosity
θ: dimensionless temperature in wall boundary layer
ϑ: dimensionless temperature in free boundary layer
ψ: dimensional stream function

Ψ: dimensionless stream function
ω: parameter defined by (3.14)
ρ: density

Appendix A. The asymptotic behaviour for $\omega \to \infty$ of certain integrals occurring in Eq. (5.13)

The expansion of $\mathscr{L}_2\{K(\omega, N)\}$ for $\omega \to \infty$ is very simple if

$$K = \tfrac{1}{2}\operatorname{erfc}\left(-\frac{\omega N^2}{2}\right) - 1$$

and will not be carried out in detail here. One only has to introduce the new variable $\tilde{P} = \omega^{\frac{1}{4}}P$ under the integral sign and expand the ω-dependent part of the integrand for $\omega \gg 1$. This procedure is simple since $K(\omega, N)$ behaves exponentially if $N \to \infty$.

For

$$K(\omega, N) = \Gamma(\tfrac{3}{4})M\left(-\frac{1}{4}, \frac{1}{2}, -\frac{\omega^2 N^4}{4}\right) + \omega N^2 \Gamma(\tfrac{5}{4})M\left(\frac{1}{4}, \frac{3}{2}, -\frac{\omega^2 N^4}{4}\right) - \omega^{\frac{1}{4}}N \tag{A.1}$$

the analysis is not so trivial. Now the function K behaves algebraically if $N \to \infty$. Indeed,

$$K \sim -\frac{1}{4\omega^{\frac{3}{4}}N^3} + O(\omega^{-\frac{7}{4}}N^{-7}) \text{ if } \omega^{\frac{1}{4}}N \to \infty. \tag{A.2}$$

We now split up the integral occurring in $\mathscr{L}_2$ into two parts, $0 \to A\omega^{-\frac{1}{4}}$ and $A\omega^{-\frac{1}{4}} \to \infty$, where A is a large but fixed number. This means that in the second integral we may use the expansion (A.2). The first integral is easily seen to be $O(\omega^{-\frac{1}{4}})$ and the second can be written

$$-\frac{N^{\frac{1}{4}}e^{-\frac{N^3}{9}}}{12\omega^{\frac{3}{4}}} \int_{A\omega^{-\frac{1}{4}}}^{\infty} P^{-\frac{1}{4}}e^{-\frac{P^3}{9}} I_{\frac{1}{3}}(\tfrac{2}{9}N^{\frac{3}{2}}P^{\frac{3}{2}})dP. \tag{A.3}$$

For $\omega \to \infty$ the lower bound in (A.3) will tend to zero. The integrand, however, behaves as P^{-1} if $P \to 0$. This means that the integral occurring in (A.3) will be $\sim \ln \omega$ if $\omega \to \infty$. Omitting details we have

$$\mathscr{L}_2\{K(\omega, N)\} = -\frac{3^{\frac{1}{4}}}{24\Gamma(\frac{1}{3})} N e^{-\frac{N^3}{9}} \omega^{-\frac{1}{4}} \ln \omega + O(\omega^{-\frac{1}{4}}) \tag{A.4}$$

if $\omega \to \infty$, where K is given by (A.1).

REFERENCES

[1] T. C. Reiman and R. H. Sabersky, Laminar flow over rectangular cavities. *Int. J. Heat Mass Transfer* 11 (1968) 1083–1085.

[2] J. F. Stevenson, Flow in a tube with a circumferential wall cavity. *J. Appl. Mech.* 40 (1973) 355–361.

[3] R. E. Chilcott, A review of separated and reattaching flows with heat transfer. *Int. J. Heat Mass Transfer* 10 (1967) 783–797.

[4] G. Goosen and J. Van Ruler, *Intermittent etching: a new possibility for photochemical milling.* Proc. 9th World Conf. on Metal Finishing, Interfinish 1976, Amsterdam.

[5] J. B. Miles, *Stanton number for separated turbulent flow past relatively deep cavities.* PhD Thesis, Mech. Engng. Dept., University of Illinois, Urbana (Ill.), 1963.

[6] D. L. Fenton and R. A. White, Heat transfer in resonant cavities spanned by low speed, turbulent, shear layers. *J. Basic Engng.* 93 (1971) 455–457.

[7] O. R. Burggraf, Analytical and numerical studies of the structure of steady separated flows. *J. Fluid Mech.* 24 (1966) 113–151.

[8] A. K. Runchal, D. B. Spalding and M. Wolfshtein, Numerical solution of the elliptic equations for transport of vorticity, heat, and matter in two-dimensional flow. High-speed comp. in fluid dynamics. *The Physics of Fluids Supplement II* (1969) 21–28.

[9] G. K. Batchelor, On steady laminar flow with closed streamlines at large Reynolds number. *J. Fluid Mech.* 1 (1956) 177–190.

[10] F. Pan and A. Acrivos, Steady flows in rectangular cavities. *J. Fluid Mech.* 28 (1967) 643–655.

[11] M. Takematsu, Slow viscous flow past a cavity. *J. Phys. Soc. Japan* 21 (1966) 1816–1821.

[12] V. O'Brien, Closed streamlines associated with channel flow over a cavity. *Phys. Fluids* 15 (1972) 2089–2097.

[13] E. O. Macagno and T. K. Hung, Computational and experimental study of a captive annular eddy. *J. Fluid Mech.* 28 (1967) 43–64.

[14] K. Stewartson, On an integral equation. *Mathematika* 15 (1968) 22–29.

[15] H. K. Moffatt, Viscous and resistive eddies near a sharp corner. *J. Fluid Mech.* 18 (1964) 1–18.

[16] R. L. Haugen and A. M. Dhanak, Heat transfer in turbulent boundary-layer separation over a surface cavity. *J. Heat Transfer* 89 (1967) 335–340.

[17] J. Fox, Heat transfer and air flow in a transverse rectangular notch. *Int. J. Heat Mass Transfer* 8 (1965) 269–279.

[18] A. M. Benis, H. L. Nossel, L. M. Aledort, R. M. Koffsky, J. F. Stevenson, E. F. Leonard, H. Shiang and R. S. Litwak, Extracorporeal model for study of factors affecting thrombus formation. *Thrombos. Diathes. haemorrh.* (Stuttg.) 34 (1975) 127–144.

[19] C. G. Caro, J. M. Fitz-Gerald and R. C. Schroter, Atheroma and arterial wall shear. Observation, correlation and proposal of a shear dependent mass transfer mechanism for atherogenesis. *Proc. Roy. Soc. Lond.* B 117 (1971) 109–159.